JOURNAL OF THEORETICAL
AND APPLIED MECHANICS
47, 4, pp. 797-814, Warsaw 2009

INFLUENCE OF THE NEGATIVE AND POSITIVE JET OF WAKE ON LAMINAR-TURBULENT TRANSITION IN A BOUNDARY LAYER

Jacek Żabski
Zygmunt Wierciński
The Szewalski Institute of Fluid-Flow Machinery PAS, Gdańsk, Poland
e-mail: zw@imp.gda.pl; jaz@imp.gda.pl

In this paper, the results of experimental investigations relating to the influence of negative and positive jet of the wake on laminar-turbulent transition in the boundary layer on a flat plate are described. Using the technique of phase averaging and wavelet analysis, the investigations were carried out in an aerodynamic tunnel with a low level of turbulence in the external stream. The existence of serious differences was noted between the influence of the negative and positive jets due to strong velocity impulses appearing in the area behind the negative jet in the place of the local minimum of the velocity. However, behind the positive jet such strong disturbances appear later, not directly in the region behind the jet. These impulses do not show any signs of chaos and fortuity, therefore they should be rather classified as determined disorder. Moreover, the region of calm behind the positive jet, well-known in the literature, remains also in the area of entirely disturbed flow.

Key words: laminar-turbulent transition, influence of wakes, flat plate

1. Introduction

The wakes from blade rings are inherently connected with the internal flow in turbomachinery changing severely flow conditions through following blade rings. They particularly cause earlier inception of the laminar-turbulent transition (LTT), which affects, in turn, decidedly the friction on the surface of the blade and the heat transfer between the flow and blades.

The wake can be differently perceived, depending on the choice of the co-ordinate system, as a defect of velocity or as a jet. And so it can be treated as the defect of velocity in the absolute system of co-ordinates connected with the motionless casing of the machine, that is, the area of reduced velocity in relation to the mean velocity, while it can be seen as the jet in the system of co-ordinates bounded with the mean velocity of the flow. If the wake is cut by a moving blade (at a certain angle to it), which takes place in a fluid-flow machine, then the boundary layer on the blade is affected by a positive jet when the speed of the jet is orientated towards the surface of the blade, and by a negative jet, if the velocity of the jet is directed from the blade towards the external flow.

We can still make an additional distinction between the influence of the negative and positive jets on the pressure and suction side of the blade. The influence of the negative jet on the suction side and the positive jet on the pressure side of a blade in a rotor in the case of compressors is illustrated in Fig. 1a. It is inversely in turbines, Fig. 1b, where the positive and negative jets affect the suction and pressure side of the rotor blade, appropriately.

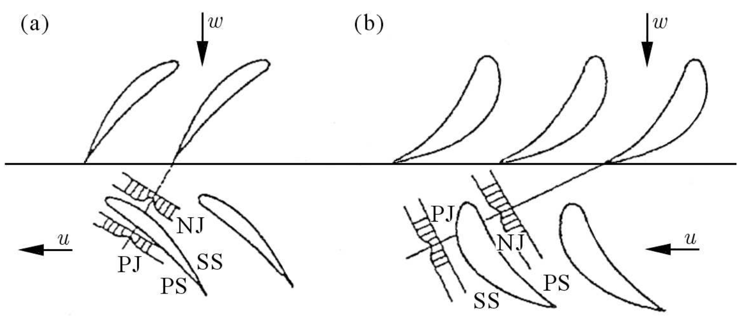

Fig. 1. Positive and negative jets of wakes in a compressor (a) and in a turbine stage (b) (Wierciński, 1999)

The question of the wakes influence on flow in the blade-to-blade passage of turbomachines has already had a long history. It will be sufficient here to mention the review work of Mayle (1991). However, many questions still remain unrecognized and, in particular, the influence of the positive and negative jet on the boundary layer and the interaction of the leading edge with a wake.

The kinematics of wake convection through a blade passage was the subject of many investigations. Meyer (1958) in his work first used the notion of jet to describe the impact of the wake on the blade surface. He distinguished the sucking and impinging effect of the jet on the plate surface. Next, Kerrebrock and Mikolajczak (1970) investigated the wake transport process in the blade-to-blade passage in the transonic compressor. The motion of the wake in the blade passage in the direction of the pressure side of the blades was the reason for the non-uniformity of the temperature field behind the stator. The above authors did not use the notion of the jet coined by Meyer (1958). In the observations made by Binder *et al.* (1984) in the experiment on a one-stage air turbine the wake was transported in the opposite direction. Probably Hodson (1985) was the first to use the words "negative jet" to describe the jet applied by Meyer to describe the feature of the wake as the difference between the mean flow and velocity defect. Most of the investigations on the wake behaviour in the blade passage were devoted to kinematics and flow structures between the blades. The impact of the impinging and sucking effects of the jet on the laminar-turbulent transition were not considered (Schobeiri and Pappu, 1997). In the paper by Addison and Hodson (1990) there is a suggestion that the negative jet has a very little effect on the boundary layer which remains either laminar or turbulent. Wierciński (1995) for the first time described the different influence of the impinging and sucking effect of the jet on the boundary layer transition. He used the designations "the positive" and "negative jet" in the description of the impinging and suction effects of the wake. In the experiment, a single rod was employed to generate a harmonic wake which coming onto the plate caused the negative and positive jet alternately. Behind the negative jet the fluctuation level is greater than the one behind the positive jet, (Wierciński, 1995, 1999). Jeon *et al.* (2002) carried out the investigation of the transition in the boundary layer on the NACA 0012 profile inserted in the squirrel cage. They reported that for the counter-clockwise rotation of the squirrel cage the wake induced turbulent patches grew more quickly and merged with each other further upstream than those for the clockwise motion of the squirrel cage. After the consideration of their experimental set up it is clear that in the terminology of the negative and positive jet it means that the earlier transition inception in the boundary layer of NACA 0012 profile appears for the negative jet. Stieger and Hodson (2005) presented the results in which the transition process in the boundary layer induced by wakes is affected by the jet that can deform the boundary layer.

There are also some papers devoted to numerical analysis of the wake convection in blade-to-blade passages, e.g. Dawes (1992), Korakianitis (1991).

Generally, in most numerical and experimental works the influence of the negative and positive jets on the LTT was not considered.

The differences in the influence of the negative and positive jet with the boundary layer in the process of laminar-turbulent transition with strong disturbances behind the negative jet were reported for the first time in the presentation by Wierciński and Żabski (2007).

The reported beneath research is aimed at investigation of the differences in the influence of positive and negative jets on the boundary layer on a plate at zero pressure gradient along it and at a low intensity of turbulence in the external stream. It is well known that the increased turbulence level is the reason for the so called by-pass transition, i.e. for overlapping when analysing the appearance of the Tollmien-Schlichting waves in the boundary layer. The understanding of the boundary affected by the jets (positive and negative) should give us some tools for better modelling of non-stationary phenomena in flow machines and the laminar-turbulent transition in particular.

2. Experimental stand and programme of investigations

The measurements were conducted in a low subsonic wind tunnel with a low level of turbulence, $Tu \leqslant 0.08\%$ and the maximum speed of flow $U = 100\,\mathrm{m/s}$. The measurement chamber with octagonal section had the following dimensions (*width*, *height*, *length*) $600 \times 460 \times 1500\,\mathrm{mm}$. The boundary layer was studied on the upper surface of the flat plate of $600 \times 700 \times 14$ (*width*, *length*, *thickness*), Fig. 2. The plate was cut at an angle $30°$ and the leading edge rounded with a radius of $2\,\mathrm{mm}$. The incidence angle of the plate was almost zero, and so the gradient of pressure close to zero value was characterised by the coefficient of acceleration $K = 7 \cdot 10^{-8}$. The boundary layer for the case of flow without wakes was laminar for almost entire length of the plate with first signs of transition further downstream than $\mathrm{Re}_x > 6 \cdot 10^5$. A round rod of $3\,\mathrm{mm}$ diameter and $600\,\mathrm{mm}$ length served as the wake generator. The rod was placed at the end of a rocker arm of length $190\,\mathrm{mm}$ (four bar linkage) and moved up and down with frequency $f = 4\,\mathrm{Hz}$, which gives the period $0.25\,\mathrm{s}$ for one negative and one positive jet. The time-phase of the rod motion generating the negative jet was recorded and the moment of time was chosen as the phase mark, when the axis of the rod was at the same height as the leading edge of the plate. At this place, the velocity of rod is about $2.6\,\mathrm{m/s}$. The upstream distance between the rod and leading edge is equal to $L = 86\,\mathrm{mm}$, so the ratio $L/d \approx 28.7$. While the phase mark is being recorded, the wake produced by the rod moves at the flow speed, so the trace of negative jet is delayed in relation to the phase mark (on wavelet graphs – perpendicular bright lines). The more distant is the traverse from the leading edge, the more delayed is the registered trace with respect to the phase mark.

The measurements were carried out by means of the StreamLine termoanemometry system with the StreamWare 3.41.20 software and the probe 55P15 of DANTEC. The data was sent to the computer by the acquisition card NI 6040E. The measurements were accomplished for the air velocity coming

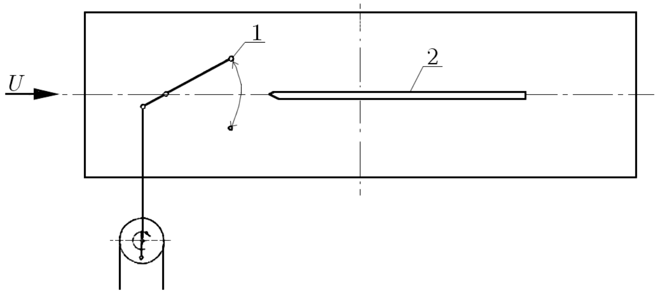

Fig. 2. Experimental stand, 1 – rod in motion as a wake generator, 2 – plate

on the plate $U = 15\,\mathrm{m/s}$, at the zero incidence angle and for eight various distances from the leading edge $x = 165$, 215, 255, 295, 325, 365, 560 and 650 mm, which corresponds to the Reynolds numbers $\mathrm{Re} = 168843$, 216979, 257412, 298640, 334414, 374159, 587243, 686918. The measurements of the velocity profiles were as a rule performed in a relatively great number of points from 110 to 160 across the boundary layer (perpendicular to the plate surface).

The velocity registration at every point took $t = 10\,\mathrm{s}$ and was sampled at frequency $f = 5\,\mathrm{kHz}$. The final distance of the last point of the velocity profile from the plate surface was determined by means of the so-called hydraulic zero method. The time-averaged velocity profiles were determined first, other parameters characteristic for the boundary layer, such as the thickness of the layer δ, the coefficients of local friction C_f and so on, were derived as well. The use of the so-called phase-averaging procedure was a farther step in the investigation. Single periods of the velocity ensemble were put one on another and the averaging along the matching points was calculated. Thus, it was possible to obtain a single period of velocity time trace with lesser random disorders of duration equal to $t = 0.25\,\mathrm{s}$. The next point of the study involved wavelet analysis using the Meyer wavelet.

3. Investigation results

3.1. Time and phase averaged

The investigation of the boundary layer started with time averaged measurements which yielded results comparable with those presented in the work by Wierciński (1999) and Kaiser (2005). The distribution of the local friction coefficient C_f is presented below as an example, Fig. 3. In Figs. 4, 5 and 6, the phase averaging outputs are presented. They are time traces of velocity in three sections corresponding to the following Reynolds numbers $\mathrm{Re}_x = 168843$, 334414 and 686918. The traverses refer to the first, fifth and eighth point in Fig. 3.

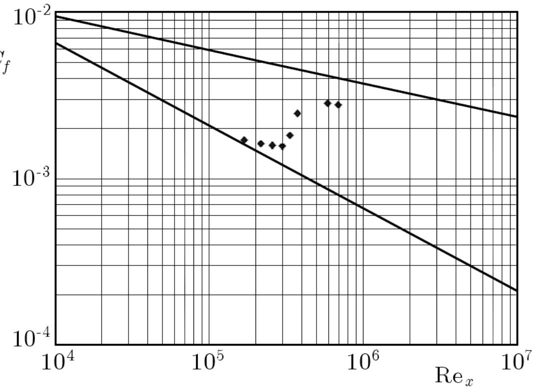

Fig. 3. Distribution of the local shear stress coefficient C_f versus Re_x

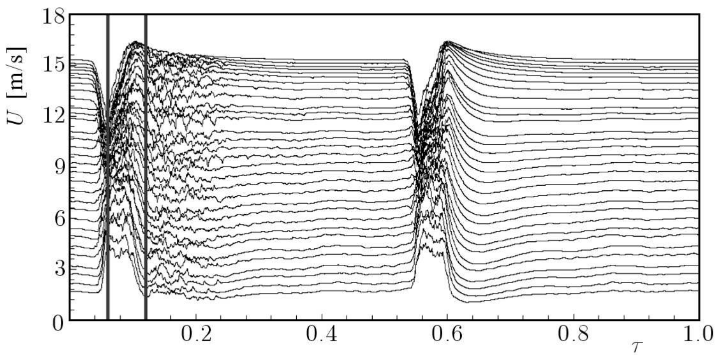

Fig. 4. Phase averaged time traces of velocity, $\mathrm{Re}_x = 168853$

To make the visual perception easier, some of the lines were removed, especially those lying outside the boundary layer, some in the mid region and these lying close to the wall, where the thermal influence of the plate was observed. Time on these graphs is dimensionless t/T, where T is the period of jets equal to $T = 0.25\,\mathrm{s}$. There are two strong velocity defects - considered from left to right are negative and positive jets, respectively. For $\mathrm{Re}_x = 168843$, Fig. 4, at the very beginning of transition the time traces are of a smooth shape, though some disorders appear just behind the negative jet. Further, for $\mathrm{Re}_x = 334414$ (Fig. 5). the zone of disorders widened within the

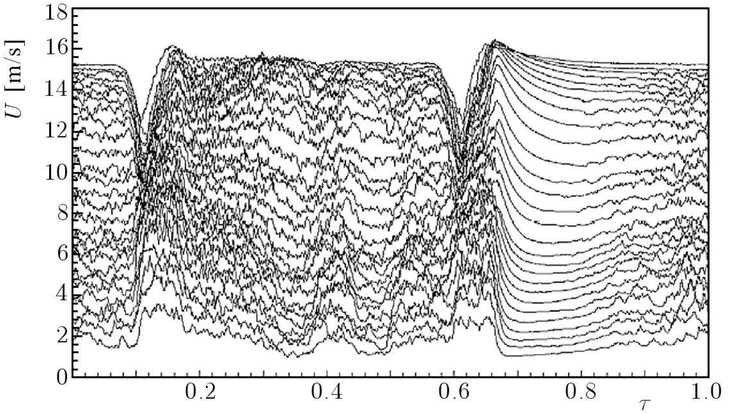

Fig. 5. Phase averaged time traces of velocity, $\mathrm{Re}_x = 334414$

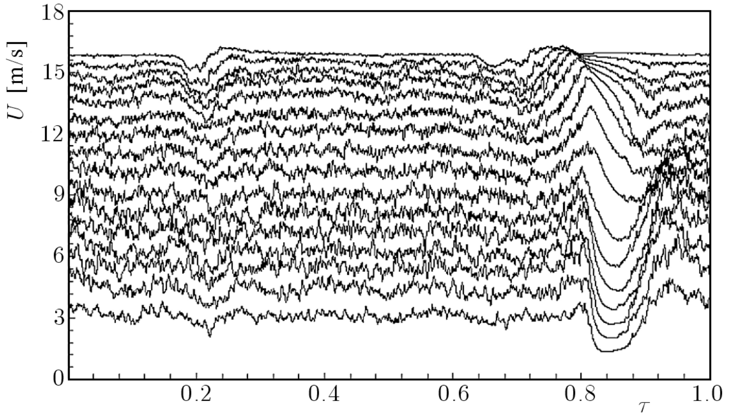

Fig. 6. Phase averaged time traces of velocity, $\mathrm{Re}_x = 686918$

whole range of time between the negative and positive jet. It looked different between the positive and negative jet. There is a becalmed region spreading from the positive jet to almost the middle of the time distance between the jets. Finally, one deals with a fully turbulent flow, Fig. 6, when the negative jet is hardly visible and the positive one holds on. The becalmed region behind the positive jet also persists, but it is rather short. The phase averaging could decrease the overall level of fluctuations and smoothed the traces but it was impossible to damp the fluctuations to zero, especially behind the negative jet where the disorder was not fully chaotic.

What can be immediately noticed at the first glance is the difference between the velocity character behind the negative and positive jet. The velocity time traces reveal much smoother character behind the positive jet, whereas behind the negative jet they are much more disturbed, Figs. 4 and 5. This can provide an evidence that the negative jet has a much stronger influence on the process of turbulence inception in the boundary layer than the positive one. In the third of these figures, i.e. in Fig. 6, the turbulent flow can be seen in its full shape and beauty. All the time the traces are disturbed, the negative wake is hardly visible – it washes away in the surrounding turbulence. It is interesting, however, that the positive wake lasts continually and the time traces clearly become smooth in the becalmed region, there are no high frequency fluctuations on the declining part of the trace behind the positive jet. It looks like a trial to return to the laminar flow.

Continuing the analysis of the flow change in the boundary layer in relation to the phase movement – the oncoming wakes – one can raise the question: what would the phase averaged velocity profile be like at a different moment of non-dimensional time, such as different sections in Figs. 4-6? Only two of them – from among many – are presented here, see Figs. 7 and 8. They are put in an order corresponding to the two thick straigth lines in Fig. 4, i.e. for the moments of the non-dimensional time $\tau = 0.06$ and 0.12. Obviously, they are not simple time averaged velocity profiles, but the phase averaged velocity profiles in two different moments of time. A large diversity of velocity profiles is visible as a function of the time phase .

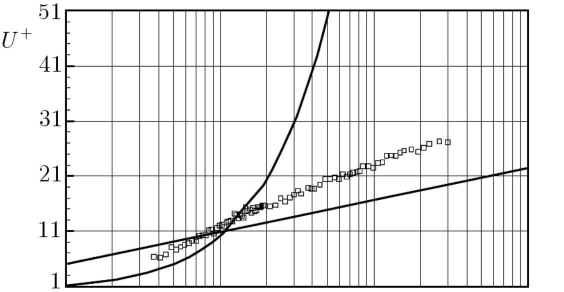

Fig. 7. Temporary velocity profile for $\mathrm{Re} = 168843$ and $\tau = 0.06$

In Fig. 7, the character of the velocity profile is turbulent. It is hard to mark a viscous sublayer according to the equation $U^+ = y^+$. It can be said that the range of the wall law $U^+ = A\ln(y^+) + B$ reaches deeper, much closer to the wall. Another conclusion can be drawn from Fig. 8, namely, the flow is laminar. The linear range exists but its course is in agreement with the following relation $U^+ = Ky^+$, where $K \neq 1$.

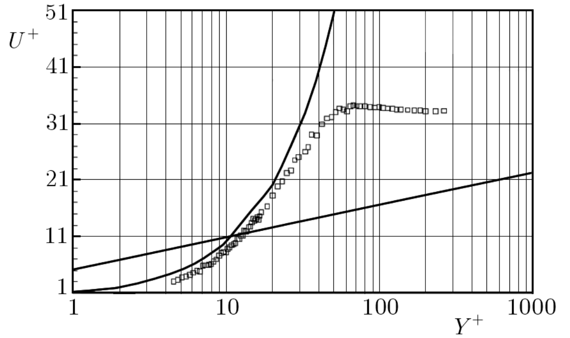

Fig. 8. Temporary velocity profile for $\mathrm{Re} = 168843$ and $\tau = 0.12$

In the next part of the report the graph of the local friction coefficient C_f versus phase time τ is shown. Dependence $C_f = f(\tau)$ was introduced in Fig. 9 for the Reynolds number $\mathrm{Re}_x = 686918$, i.e. for the last investigated point where the flow is almost fully disturbed by turbulence, whereas in Fig. 10 the graphs of $C_f = f(\mathrm{Re}, \tau)$ for three various Reynolds numbers $\mathrm{Re}_x = 168843$, 298340 and 686918 are presented. The spread of changes of the C_f coefficient evidently rises with the increasing Reynolds number, and for $\mathrm{Re}_x = 168843$ it oscillates around the value for the laminar flow. Then, for the Reynolds number $\mathrm{Re}_x = 686918$ the range of changes becomes considerably larger because it passes from laminar to the turbulent values and attains its maximum somewhere above. Connecting successive values of C_f from each measuring section (approximately for one value of the Reynolds number), it is possible to obtain two full loops, one for the negative and the other for the positive jet.

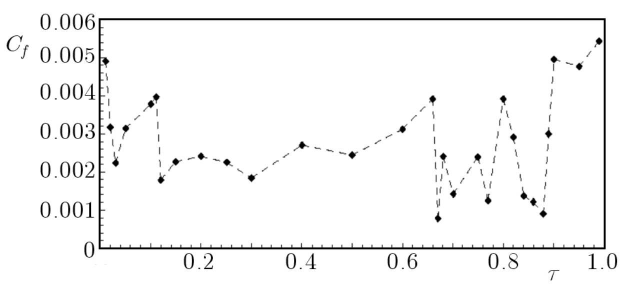

Fig. 9. Local friction coefficient $C_f = f(\tau)$ for $\mathrm{Re}_x = 686918$ versus phase time

In the next part of the report the measurement results of the velocity fluctuation across the boundary layer are presented. In one graph they illustrate both fluctuations measured as time averaged and as phase averaged. The difference between the time and phase averaged values can be treated as a random part of the velocity fluctuation like turbulence. Figure 11 shows the above discussed parts of velocity fluctuations for $\mathrm{Re}_x = 168853$, whereas Fig. 12 for $\mathrm{Re}_x = 686918$.

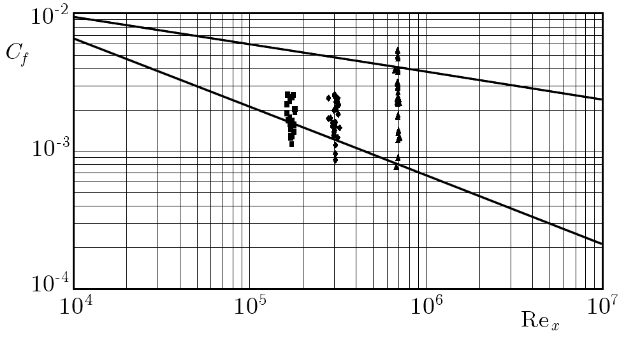

Fig. 10. Local friction coefficient $C_f = f(\tau)$ for $\mathrm{Re}_x = 168843$, 298640 and 686918

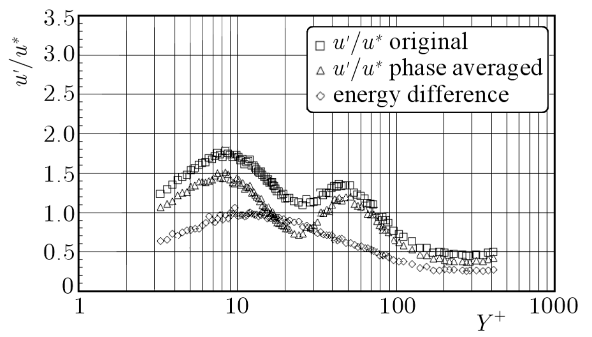

Fig. 11. Distribution of velocity fluctuations for: $\mathrm{Re}_x = 168853$: time and phase averaged and turbulent

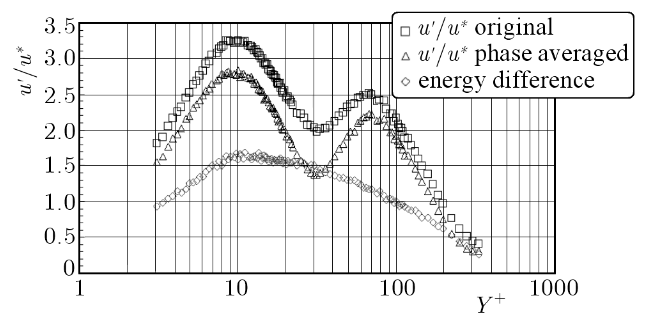

Fig. 12. Distribution of velocity fluctuations for: $\mathrm{Re}_x = 686918$: time and phase averaged and turbulent

As can be expected, the level of turbulent fluctuations is higher for the Reynolds number Re = 686918 (Fig. 12) than for Re = 168853 (Fig. 11) because the turbulization process of the flow proceeds together with the growth of the Reynolds number. But simultaneously, the amplitude of phase averaged fluctuations grows, which can be connected with the process of wake widening, although in general, the amplitude of velocity in a wake gets smaller if widening occurs. Another attempt to explain this process, however, is a possibility of amplification in the boundary layer.

3.2. Results of wavelet analysis

It is well known that the wavelet analysis is particularly useful for nonstationary signal analysis, where one deals with signals of different frequencies at different time intervals. The feature of wavelet analysis is crucially different from the Fourier analysis, where it is necessary to assume that the analysed signal is stationary.

Five points in the velocity fluctuation profile were chosen to carry out the wavelet analysis, i.e. two points lying at the edges of the distribution and three characteristic points of the distribution of the velocity fluctuation, two maximal and one local minimum. The point at the outside edge of the distribution goes beyond conventional borders of the layer, that is $U = 0.99U_0$, because the velocity fluctuations are well seen outside this border, and this point denotes the area where the velocity fluctuation does not become smaller any more and are actually equal to the velocity fluctuation in the outside stream. It is obvious that the points could be found in a different way. However, in this paper, for the presentation purpose only one point was chosen as closest to the plate surface where the thermal influence of the plate on the velocity measurements was not observable, so it is usually the point in the range of $y^+ = 10$-13.

The following seven graphs were presented for the subsequent Reynolds numbers. Every graph is built in a similar way. The velocity time trace is presented in the first subgraph at the top, usually somewhat above three periods of the wake. The second central subgraph shows the results of the wavelet analysis of the records from the first subgraph, thus the values of wavelet coefficients a for a given frequency and time. The graph is three-dimensional but the altitudes are given as isoheights in shades of grey with shade bar with scale on the right side. They are vertical bright lines in the figures. Every line points out a negative jet. Among negative jets, there are obviously positive ones. The bright horizontal line denotes the frequency $f = 192$ Hz. The values of wavelet coefficients for this frequency are introduced in the third lowest subgraph. The wavelet coefficents a are indicated on the vertical axis of this graph, whereas the time t is given on the horizontal axis like in the two preceding graphs.

In the first of these graphs, Fig. 13, it is possible to see some considerable velocity distortions in the time-interval just after passing the negative jets in the form of a series of velocity impulses, usually two or three velocity disturbances. Such disturbances are not observed behind the positive jets. They appear behind the negative jet in the area of the local velocity minimum. Moreover, two characteristic wave trains of frequencies $f = 42\,\mathrm{Hz}$ and $192\,\mathrm{Hz}$ in the time-intervals between wakes are seen. The intensity of the wave of frequency $192\,\mathrm{Hz}$ is considerably larger behind the negative jets than the positive one, which can be observed in the third subgraph, Fig. 13. The second wave of frequency $42\,\mathrm{Hz}$ in principle appears with practically equal intensity behind both negative and positive jets.

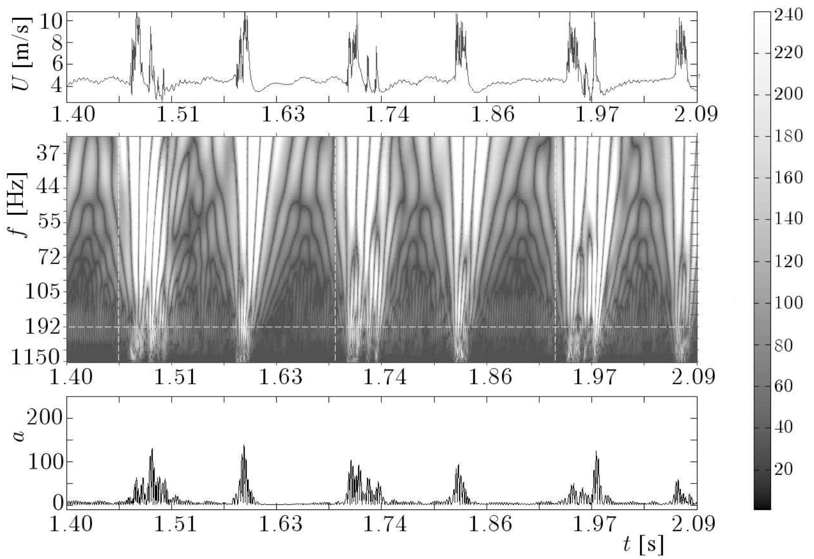

Fig. 13. Wavelet chart, $\mathrm{Re}_x = 168843$, $Y^+ = 10$

In Fig. 14, for $\mathrm{Re} = 216979$, the increasing disturbances behind the negative jet can be seen, and apart from single impulses also a series of impulses is practically bounded with each other. Moreover, some intensive impulses of velocity occur in the area close to the half of the range between the negative and positive jets, which seems to be novel, and the impulses are not tied up with the impulses behind the negative jet alike. The intensity of the wavelet coefficients for the frequency $f = 42\,\mathrm{Hz}$ diminishes, while the occurrence of wave-trains about the frequency $f = 192\,\mathrm{Hz}$ widens.

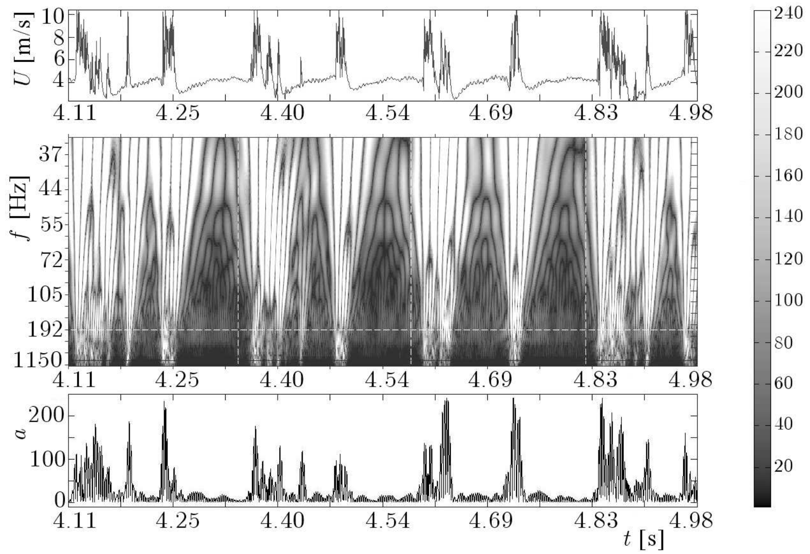

Fig. 14. Wavelet chart, $\mathrm{Re}_x = 216979$, $Y^+ = 10$

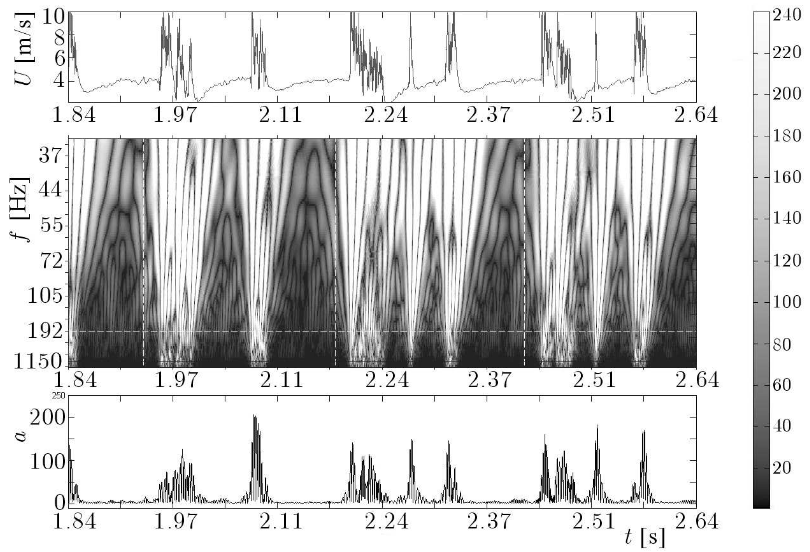

Fig. 15. Wavelet chart, $\mathrm{Re}_x = 257412$, $Y^+ = 10$

In Fig. 15, with respect to the Reynolds number $\mathrm{Re} = 257412$, one can observe that the intensity of impulses behind the negative jets grows, like the intensity of a single impulse in the half of the area behind some negative jets. The level of disturbances behind the positive jets is still small, and the becalmed region is especially well visible. However, some disturbances begin to appear before the negative jets and the intensity of these disorders – as will be seen farther – will rise.

In Fig. 16, regarding the Reynolds number $\mathrm{Re} = 298640$, a farther growth of disturbances past the negative jets can be easily noted, and even the first large impulses of the velocity appear on the background of the increasing level of disturbances in the area before the positive jets. Nevertheless, there is another region without disturbances directly behind the positive jet. Thus, the zone called the becalmed region remains firm. The described symptoms can, of course, be observed in the three diagrams. In the upper diagram the time traces show the number of impulses continuously increasing, whereas in the central diagram the full wavelet spectrum from 32 to 1050 Hz illustrates the rising number of distortions. Finally, in the third diagram, a section for frequency $f = 192$ Hz also shows a larger level of disturbances.

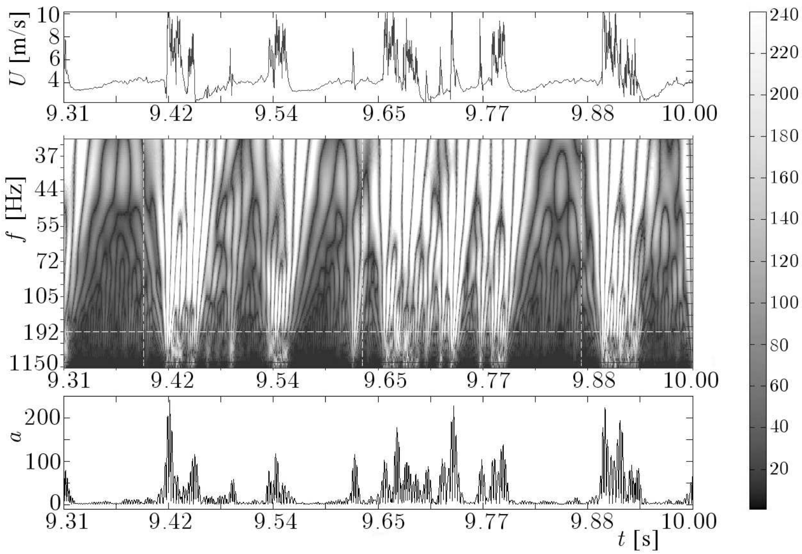

Fig. 16. Wavelet chart, $\mathrm{Re}_x = 298640$, $Y^+ = 10$

In Fig. 17, for the Reynolds number $\mathrm{Re} = 334414$, the tendencies described for Fig. 16 keep on, that is, the number of strong velocity impulses grows behind the negative jets. The becalmed region behind the positive jets still holds and the number of strong impulses before negative jet rises.

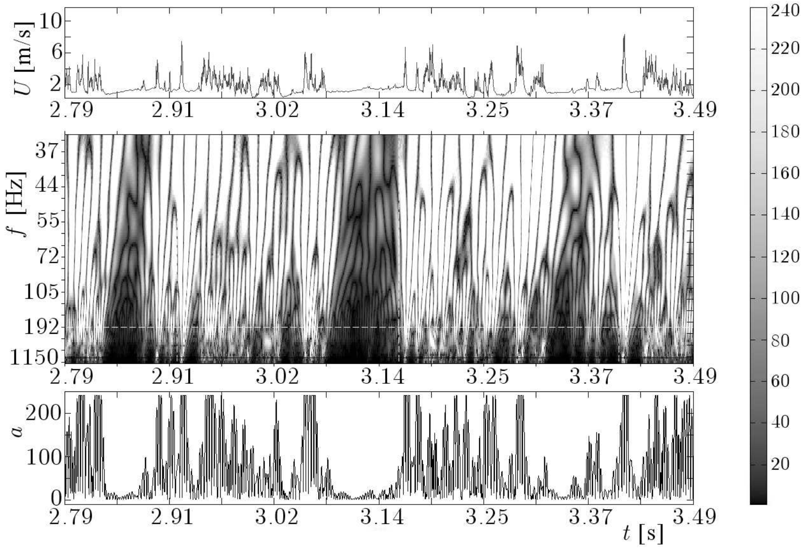

Fig. 17. Wavelet chart, $\mathrm{Re}_x = 334414$, $Y^+ = 10$

Furthermore, in Figs. 18 and 19 for the Reynolds numbers $\mathrm{Re} = 374159$ and 686918, the area behind the negative jets is entirely filled with strong impulses of the velocity, whereas the emphasised becalmed region past the positive jet holds on.

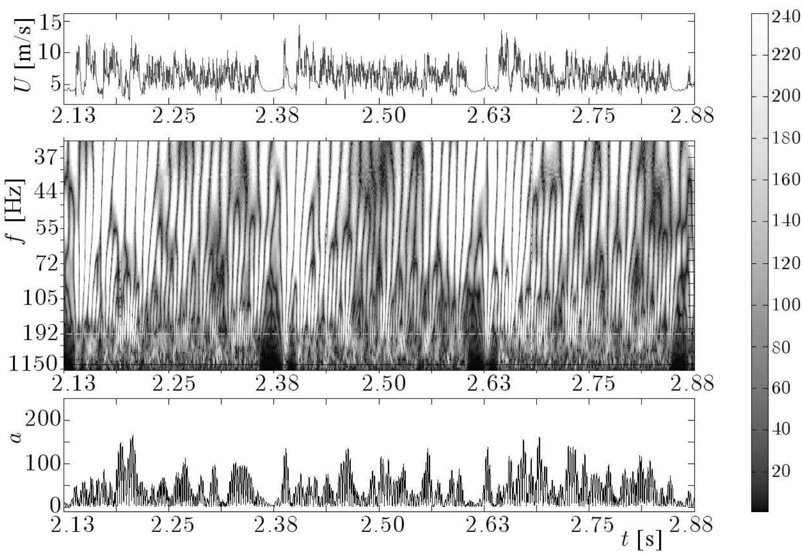

Fig. 18. Wavelet chart, $\mathrm{Re}_x = 374159$, $Y^+ = 12$

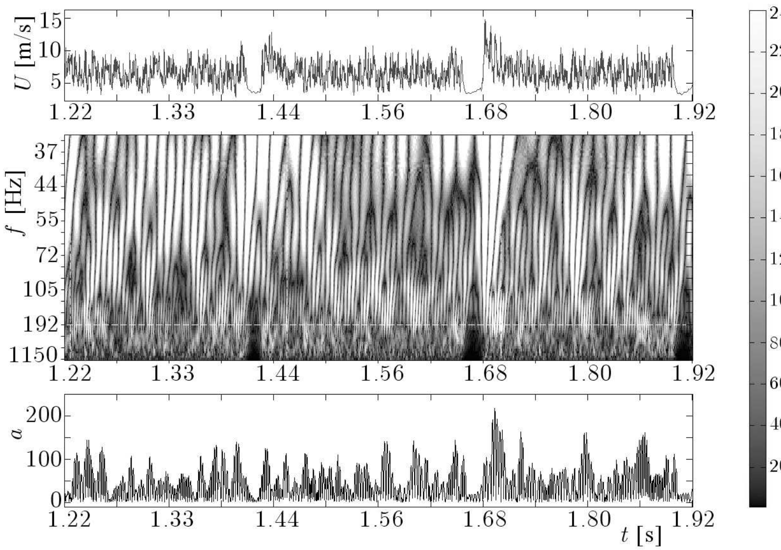

Fig. 19. Wavelet chart, $\mathrm{Re}_x = 686918$, $Y^+ = 12$

4. Conclusions

The results of the experiment presented in the work show a fundamental difference of the influence of the negative and positive jet on the boundary layer. A strong distortion in the form of velocity impulses is revealed in the area just behind the negative jet for the lowest value of the Reynolds number measured in the experiment. These disturbances are observed in the region of the local minimum of velocity. The decrease of the pressure in the negative jet can be very likely responsible for the appearance of these disturbances. There are no such disturbances behind the positive jet which can be explained by the pressure rise in the positive jet. With the growing Reynolds number, the quantity of these impulses grows and they join in larger structures, the most probably in the spots of turbulence, but they clearly still differ from the jet (wake). It is possible to say that the character of these disturbances is not entirely chaotic and rather deterministic.

Next, the impulses of velocity appear suddenly in the half of the distance between the negative and positive jet. Their character can be supposed as the turbulent spot of natural transition probably not connected with the influence of wakes (jets). However, the becalmed region, which is distinctively visible behind the positive jet still holds on, whereas such a becalmed region passes unnoticed behind the negative jet. The more the zone behind the negative jets is filled up with strong impulses, the greater is the Reynolds number. Thus the becalmed region persists in the final Reynolds number reported in the present work.

Additionally, the harmonic wave trains of frequencies of $f = 42$ and $192\,\mathrm{Hz}$ in the regions between both jets are observed. And these wave trains are not visible outside the boundary layer.

Moreover, the measurements of the distribution of the phase averaged velocity across the boundary layer show that the viscous sublayer is probably much smaller in the area of the wake than in the turbulent boundary layer without wakes. Furthermore, beyond the area of the wake, even if the laminar boundary layer of the linear type $U^+ = Ky^+$ is considered, the coefficient K is rather different from unity.

References

1. Addison J.S., Hodson H., 1990, Unsteady transition in an axial-flow turbine: Part 2-Cascade Measurements and Modeling, *ASME Journal of Turbomachinery*, **112**, 215-221
2. Binder A., Forster W., Kruse H., Rogge H., 1984, An experimental investigation into the effect of wakes on the unsteady turbine rotor flow, *ASME Journal of Engineering for Gas Turbines and Power*, **107**, 1039-1046
3. Dawes B., 1992, The simulation of three dimensional viscous flow in turbomachinery geometries using a solution-adaptive unstructured mesh methodology, *ASME Journal of Turbomachinery*, **114**, 528-537
4. Hodson H.P., 1985, Measurements of wake generated unsteadiness in the rotor passage of axial flow turbines, *ASME Journal of Turbomachinery*, **107**, 467-475
5. Jeon W.-P., Park T.-C., Kang S.-H., 2002, Experimental study of boundary layer transition on an airfoil induced by periodically passing wake, *Experiments in Fluids*, **35**, 229-241
6. Kaiser M., 2005, *Analogia wymiany ciepła i pędu przy niestacjonarnym opływie płyty*, PhD thesis, Gdańsk
7. Kerrebrock J.L., Mikolajczak A.A., 1970, Intra-stator transport of rotor wakes and its effect on compressor performance, *ASME Journal of Engineering for Power*, **92**, 359-368
8. Korakianitis T., 1991, On the propagation of viscous wakes and potential flow in axial-turbine cascades, *ASME Paper No. 91-GT-373*
9. Mayle R.E., 1991, The role of laminar-turbulent transition in gas turbine engines, *J. Turbomachinery*, **113**, 509-537

10. Meyer R.X., 1958, The effects of wakes on the transient pressure and velocity distributions in turbomachines, *Trans. Journal of Basic Engineering*, **80**, 1544-1552
11. Schobeiri M.T., Pappu K., 1997, Experimental study on the effect of unsteadiness on boundary layer development on a linear turbine cascade, *Experiments in Fluids*, **23**, 306-316
12. Stieger R.D., Hodson H.P., 2005, The unsteady development of a turbulent wake through a downstream low pressure turbine blade passage, *ASME Journal of Turbomachinery*, **127**, 388-394
13. Wierciński Z., 1995, The influence of the periodic wake behind pendulating in the cross stream direction on the laminar-turbulent transition in the boundary layer of a flat plate, In: *Unsteady Aerodynamics and Aeroelasticity of Turbomachinee*, Elsevier, Amsterdam, 461-479
14. Wierciński Z., 1999, *Przejście laminarno-turbulentne w warstwie przyściennej indukowane śladami spływowymi*, IMP PAN, ZN 499/1450/99, Gdańsk, DSc Thesis
15. Wierciński Z., Żabski J., 2007, Phase averaged characteristics of the boundary layer in transition induced by wakes, *Workshop on Transition Modelling and Turbulent Combustion*, Ghent, November 29-30
16. Wierciński Z., Żabski J., 2008, Investigation of the negative and positive jets in the induced by wakes transition, *5th. European Congress on Computational Methods in Applied Sciences and Engineering (ECCOMAS 2008)*, Venice, Italy

Wpływ ujemnego i dodatniego strumienia śladu spływowego na przejście laminarno-turbulentne w warstwie przyściennej

Streszczenie

W pracy przedstawiono badania eksperymentalne dotyczące wpływu ujemnego i dodatniego strumienia śladu spływowego na przejście laminarno-turbulentne w warstwie przyściennej na płaskiej płycie. Badania przeprowadzono w tunelu aerodynamicznym o niskim poziomie turbulencji przepływu zewnętrznego, wykorzystując technikę fazowego uśredniania i analizy falkowej. Stwierdzono istnienie poważnych różnic między oddziaływaniem ujemnego i dodatniego strumienia w postaci silnych impulsów prędkości pojawiających się w obszarze za ujemnym strumieniem w miejscu o lokalnego minimum prędkości. Za dodatnim strumieniem takie silne zaburzenia pojawiają się później i nie bezpośrednio za nim. Ponadto regiony uspokojenia za dodatnim strumieniem, dobrze znane z literatury, są dobrze widoczne także w rejonie całkowicie zaburzonego przepływu.

Manuscript received July 10, 2008; accepted for print May 11, 2009